PAPER

Seeing the invisible: XRF reveals lead distributions in coral organisms grown in the Red Sea (Gulf of Aqaba)†

Katrein Sauer, [ID] [a] Maayan Neder, [ab] Ivo Zizak, [ID] [c] Paul Zaslansky [ID] *[d] and Tali Mass [ID] *[a]

Lead (Pb) contamination in marine ecosystems poses a significant ecological threat. Not much is known about its effects on coral reefs, which serve as vital biodiversity hotspots and climate refuges. This study revealed bioaccumulation of Pb in the organism of two stony coral species, *Stylophora pistillata* and *Pocillopora verrucosa*, widely studied in the Gulf of Aqaba. Microfocus X-ray fluorescence (XRF) imaging revealed widespread accumulation of Pb within the coral tissues but not in the skeletons. The finding that Pb predominantly accumulates in the soft tissues with no evidence of Pb in the mineral suggests that exposure was short or of low concentration. Both highlight the great sensitivity of coral organisms to Pb uptake, with likely negative impacts on the organism. We suggest that anthropogenic Pb contamination, intensified by factors such as urban runoff or industrial discharges, still poses a serious risk to coral health and resilience despite years of efforts to curb exposure. Future research should focus on the kinetics of Pb bioaccumulation, effects of short-term *versus* long-term exposure and the combined effects of heavy metals and temperature on coral physiology.

Introduction

Scleractinian corals are crucial to marine ecosystems, serving as the foundation of shallow-water tropical reefs that support immense diversity and productivity.[1] Beyond their ecological importance, these corals provide structural, social, and economic roles. However, they are increasingly threatened by anthropogenic

[a]*Department of Marine Biology, The Leon H. Charney School of Marine Sciences, University of Haifa, 199 Abba Khoushy Ave., Mount Carmel, Haifa 3103301, Israel. E-mail: tmass@univ.haifa.ac.il*

[b]*The Interuniversity Institute of Marine Sciences, Eilat 88103, Israel*

[c]*Helmholtz-Zentrum-Berlin, Department for Structure and Dynamics of Energy Materials (SE-ASD), Albert-Einstein-Straße 15, 12489, Berlin, Germany*

[d]*Charité – Universitätsmedizin Berlin, Department for Operative, Preventive and Pediatric Dentistry, Aßmannshauser Straße 4-6, 14197, Berlin, Germany. E-mail: paul.zaslansky@charite.de*

† Electronic supplementary information (ESI) available. See DOI: https://doi.org/10.1039/d5fd00024f

impact,[2] such as increased temperatures due to the evolving climate crisis and ocean acidification.[3,4]

Already more than six decades ago, the harmful effects of Pb on marine organisms were identified,[5] which led to a global movement to eliminate the use of leaded fuel.[6] Japan took the initiative in 1970 by limiting tetraethyl Pb in gasoline,[7] followed by similar measures in the United States and the introduction of catalytic converters,[8] which required unleaded gasoline to function properly. These efforts expanded globally through the United Nations Environment Programme (UNEP) which successfully ended the use of leaded gasoline worldwide in 2021, with Algeria being the last country to comply.[9]

As a result, the major issue of Pb poisoning seemed to be resolved, and focus has shifted to other threats such as ocean acidification, ocean warming and microplastic pollution.

Pb is a non-biodegradable heavy metal that persists in soil, air, and aquatic environments, and remains a significant component of the oceanic Pb cycle.[10,11] Once introduced into the marine environment, Pb occurs in ionic or organically complexed manifestations within seawater.[12,13] Predominant forms include salts ($PbCO_3$, $Pb(NO_3)_2$, $Pb(SO_4)$), hydroxylated ($Pb(OH)_2$), or ionized (Pb^{2+}) forms. The bioavailable Pb^{2+} ion readily forms complexes with both organic and inorganic ligands. Organic Pb complexation often involves Ca^{2+}, Mg^{2+} and Zn^{2+},[14,15] while inorganic complexation is dominated by chloride and carbonate.[16] Although only a small portion of Pb remains dissolved and bioavailable in seawater, this fraction can enter the marine food web and affect organisms such as corals.[17]

The persistence of oceanic Pb has been demonstrated in the Gulf of Aqaba (GoA) by measurements of dissolved Pb concentrations and isotopic compositions. In October 2018, dissolved Pb concentrations ranged from 19 to 85 pmol kg^{-1} (0.004 to 0.02 µg L^{-1}), with isotopic ratios of $^{206}Pb/^{207}Pb$ and $^{208}Pb/^{206}Pb$ reported between 1.163–1.190 and 2.062–2.093.[18] Note that these levels are below the critical threshold level of 2 µg L^{-1} established by the Australian Water Quality Guidelines for marine environments.[19]

Pb accumulation in marine organisms can result in concentration levels that are several orders of magnitude higher than those found in the surrounding water.[20] Aquatic invertebrates are known to take up and accumulate trace metals, whether essential or toxic.[21] Indeed, previous studies have demonstrated that Pb can accumulate in both coral tissue and skeleton.

To date, different analytical approaches for determining Pb accumulation in coral skeletons have provided controversial results, indicating limitations and inconsistencies associated with extraction methods and analytical techniques.[22] Methods such as laser ablation inductively coupled plasma mass spectrometry (LA-ICPMS) have been used to trace Pb contamination,[23] however, this technique often averages Pb concentrations across entire samples, which limits its resolution and the ability to localize Pb accumulation with high detail. Similarly, bulk analysis techniques such as optical emission spectrometry (OES) and flame atomic absorption spectrophotometry (FAAS) have been employed to detect Pb contamination in both modern and fossil coral skeletons.[24] While these methods can quantify Pb concentrations, they offer low resolution, making it difficult to resolve specific regions where Pb accumulates. These constraints highlight the need for high-resolution techniques to better understand the spatial distributions of Pb within coral skeletons and tissues.

In this study, we present observations of corals cultured in the open aquaria of the Gulf of Aqaba, and we report on observations of distributions of Pb in relation to the coral tissues and the skeletons. To do so, we make use of microfocus X-ray mapping combined with X-ray fluorescence (XRF) to provide detailed insights into the distribution and presence of environmental Pb within marine ecosystems.

Experimental

Coral nubbin collection and preparation

Nubbins from two genotypes of the stony corals *Stylophora pistillata*[25] ($n = 3$) and *Pocillopora verrucosa*[26] ($n = 5$) were collected under a permit granted by the Israel Nature and Parks Authority (permit number 2019/4210). The ~1 cm nubbins of coral branches (ESI Fig. 1a and b†) were harvested from a depth of 5 m near the Interuniversity Institute for Marine Science (IUI) at the Gulf of Eilat, northern Red Sea (29° 30′ N, 34° 56′ E). Each nubbin was attached using superglue to the inner surface of polymethyl methacrylate (PMMA) cylinders (1.5 cm diameter, ESI Fig. 1c†).

The nubbins were cultivated for approximately one month in an open aquarium connected with the flow-through seawater system at the IUI. The system operated under ambient water temperature and a natural light condition. Seawater was continuously supplied *via* a pump positioned at a depth of 30 meters in the Red Sea, with delivery ensured through PVC pipelines. During this time, the corals adapted and formed new tissue and skeleton at the base of the cylinders (ESI Fig. 1d,† marked by black arrows), indicative of thriving and healthy growth. Once the nubbins exhibited significant amounts of new skeleton formation while starting to cover the entire bottom of the cylinder, they were fixed in a solution containing 2% paraformaldehyde and 0.05 M sodium cacodylate buffer in 22 g per L Na_2CO_3 for 1 h in order to preserve the soft tissue for further analysis.

Following fixation, the samples were washed twice with 0.05 M sodium cacodylate buffer in 22 g per L Na_2CO_3 for 5 min each and subsequently dehydrated in graded ethanol solutions (50%, 60%, 70%, 80%, and 90% anhydrous ethanol with 1 g per L Na_2CO_3). The dehydration process concluded with two washes in 100% anhydrous ethanol. The samples were then embedded in EpoFix resin (agar scientific # AGB8790) and sectioned into 300 μm thick slices.

Scanning electron microscopy (SEM)

Uncoated 300 μm thick sections from coral nubbins of *Stylophora pistillata* ($n = 8$) and *Pocillopora verrucosa* ($n = 11$) were imaged using a scanning electron microscope (SEM, PhenomXL, ThermoFisher, Eindhoven, Netherlands). Imaging was performed in backscatter electron mode (SEM-BEI) at an acceleration voltage of 15 kV, with a working distance of ~20 mm, to image embedded mineralized regions visible on the cross sections.

Synchrotron based X-ray fluorescence (XRF)

Synchrotron based XRF measurements were performed at the mySpot beamline of the BESSY II synchrotron light source (HZB – Helmholtz-Zentrum, Berlin,

Germany[27]). Elemental distributions within thin sections of *P. verrucosa* ($n = 11$) and *S. pistillata* ($n = 8$) were obtained by lateral raster scanning of each sample using an oval shaped X-ray beam sized 25×32 µm that created an X-ray fluorescence excitation source inside the sample. XRF spectra were collected using a 40 mm^2 silicon drift detector (Rayspec, SiriusSD, SGX Sensortech). The fluorescence detector was positioned at a 45° angle relative to the incident beam. Regions of interest were pre-identified in each sample using microscopy, and scans were performed at an excitation energy of 17 keV to generate elemental maps by moving the sample plane across the µm diameter beam. Peaks in the XRF spectra were integrated and visualized using Fiji.[28]

The generation of characteristic XRF signals depends on the excitation of atomic elements within the X-ray beam path.[29] The absorption cross-section, which reflects the probability that incident photons are absorbed, exhibits a sharp increase at the energy threshold beyond which inner-shell electrons become excited. Fluorescence occurs when the excited electrons with higher energy level fill the lower-energy vacancy, emitting characteristic X-ray photons with an energy corresponding to the difference between these levels. For Pb, such fluorescence occurs with an energy of ~10.55 keV (corresponding to the Lα_1 transition[30]). In the present study an incident beam energy of 17 keV was used, exceeding the Pb L-edge in the absorption spectrum (corresponding to 15.861 keV [31]).

Results

Pb accumulation is observed in healing and re-growing adult coral colonies

In situ X-ray fluorescence (XRF) imaging of slices from both the original and the newly growing tissues of the coral species *Stylophora pistillata* (Fig. 1a) and *Pocillopora verrucosa* (Fig. 2a) reveals significant Pb incorporation in the soft tissue regions of the coral organism. The Pb was localized in the coral tissue surrounding the skeleton and inside the polyp chambers. Two representative examples are shown: one for a mature *S. pistillata* nubbin (Fig. 1) and another for a newly formed growth region located on the outer margins of the *P. verrucosa* (Fig. 2). Both examples demonstrate that Pb accumulated in regions adjacent to the mineralized skeletons (Fig. 1b and 2b marked by white arrowheads). Thus, in all regions of newly formed material, the encasing soft tissue fluoresces with an intense signal of Pb. SEM imaging of all cross-sections confirmed that the Pb signal always arises from regions external to the mineralized mass (Fig. 1c and 2c, corresponding to perpendicular views of Fig. 1b and 2b, respectively). Elemental mapping was collected point by point yielding thousands of spectra covering 3955×2182 µm^2 (Fig. 1d–f) and 956×589 µm^2 (Fig. 2d–f) regions for the mature and newly grown edges, respectively. Calcium (Ca) (Fig. 1d and 2d) and strontium (Sr) (Fig. 1e and 2e) identify the coral skeleton in both regions, with a stronger calcium signal obtained on the surface side near the detector due to strong self-absorption in the sample bulk. Pb was always localized outside the skeletal framework, surrounding it or appearing in voids/polyps within the mineralized tissue. Pb distribution is shown in magenta (Fig. 1f and 2f), highlighting its localization in close proximity to the skeletal structure that the tissue creates.
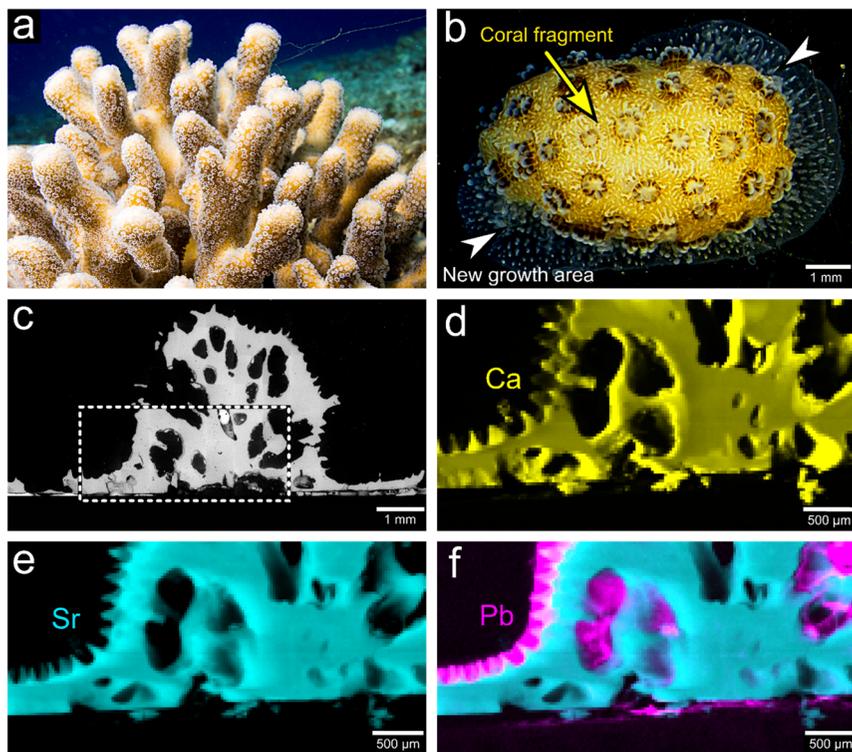
Fig. 1 *Stylophora pistillata* elemental mapping. (a) Underwater photograph of a *S. pistillata* colony in its natural habitat within the Gulf of Aqaba. (b) Light microscopy image of a *S. pistillata* nubbin after one month, showing the cylindrical coral fragment (yellow arrow) with the newly formed tissue and skeleton covering the base, indicated by white arrowheads. (c) Scanning electron microscopy (SEM) backscattered image of a thin section of the nubbin. (d–f) X-ray fluorescence (XRF) elemental maps of the boxed region in (c) showing (d) calcium (Ca) and (e) strontium (Sr) co-localized within the coral skeleton, while (f) Pb is predominantly concentrated external to the Sr layer, encasing the skeleton. Pb, even in PPM quantities, is never identified in the mineralized skeleton.

Discussion

Pb distribution in coral tissues

This study uses the high sensitivity of the X-ray fluorescence (XRF) to detect and map the distribution of Pb in stony corals cultivated in open aquaria at the IUI research station in the Gulf of Aqaba in 2020. Our observations reveal extensive Pb contamination in the coral tissues surrounding the skeleton, raising concerns about the health of these and other marine creatures in the ecosystem. XRF indicates that Pb predominantly accumulates in the soft tissues of corals and without integration into their skeletal structures. The absence of Pb traces in the skeleton suggests either a recent transient exposure, or low-grade long-term exposure. The former scenario could possibly be a result from a dust storm, or a temporary anthropogenic source.[18,32] Prolonged, low-level exposure to Pb might also load the coral with Pb, but possibly was insufficient to replace calcium in the
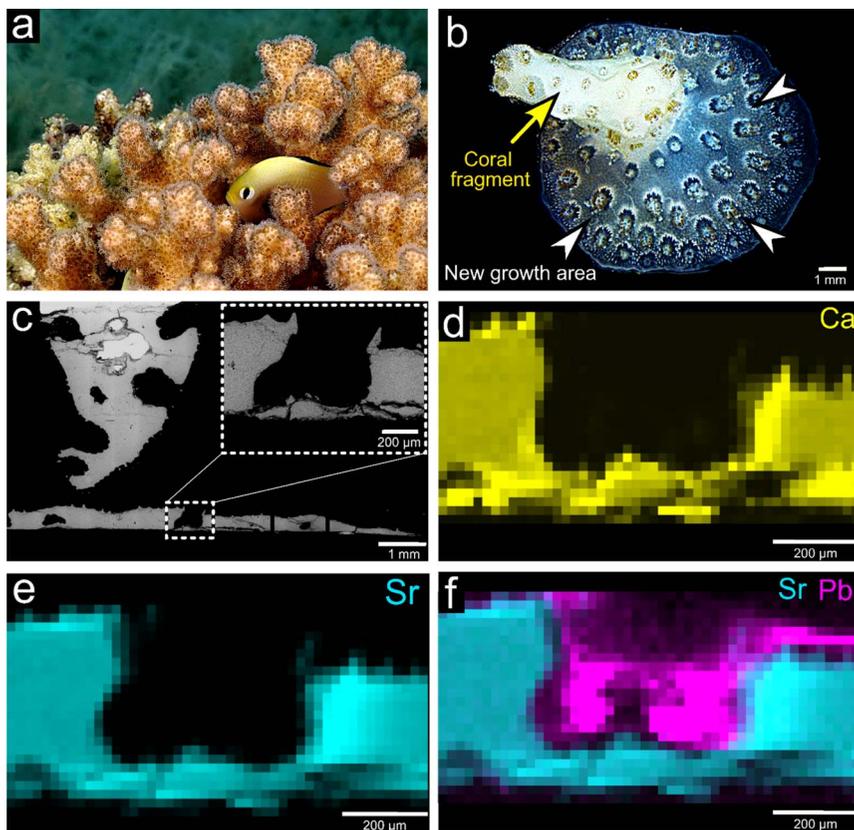
Fig. 2 *Pocillopora verrucosa* elemental maps. (a) Underwater photograph of a *P. verrucosa* colony thriving in its natural environment in the Gulf of Aqaba. (b) Light microscopy image of a *P. verrucosa* nubbin, showing the cylindrical coral fragment (marked with yellow arrow). The newly formed growth fronts covering the base and encircling the cylinder (indicated by white arrowheads) represent newly formed material. (c) SEM back scattered image of a thin section from the nubbin (top) and the inset highlighted a newly developed polyp (framed in white at the bottom). (d–f) XRF elemental maps of the polyp region outlined in the box in (c), revealing (d) Ca, and (e) Sr co-localized to the coral skeleton, whereas (f) Pb is concentrated in the non-mineralized regions, in contact with the strontium layer but exterior of the skeleton. Pb is never identified in any of the mineralized regions.

growing skeleton. The widespread contamination found in all soft tissue regions was an unexpected finding. This may indicate that the corals tolerate some degree of Pb exposure while continuing to form normal calcium carbonate structures, both amorphous and crystalline.[33]

Our findings challenge the prevailing assumption that Pb readily incorporates into coral skeletons.[24,34] Although prior studies report high concentration of heavy metals in sediments and powdered coral skeletons, our study showed no evidence of Pb integration into the new skeleton that the corals were growing. Pb removal from aqueous environments typically occurs through adsorption, surface precipitation, and incorporation into solid phases, such as calcium carbonate

surfaces. Previous reports indicate that Pb^{2+} ions are rapidly adsorbed within minutes followed by the formation of Pb carbonate minerals such as cerussite and hydro-cerussite demonstrating the capacity of calcium carbonates to act as sinks for Pb.[35]

While Pb can theoretically substitute for calcium in crystalline structures such as calcite or aragonite,[36] due to similarities in their ionic radii and competition for calcium-binding sites,[37,38] we did not observe such integration in our coral samples. This absence might reflect a short exposure period, possibly occurring not long before sample extraction, limiting the time for incorporation into the skeleton. Despite similarities, the slightly larger ionic radius of Pb^{2+} could increase binding distances,[39] potentially causing lattice distortions when substituted into crystalline structures such as calcite or aragonite. Such distortion would likely hinder efficient integration into the crystalline phase.

Note that incorporation into the amorphous calcium carbonate (ACC) phase, a precursor to skeletal formation originating within the tissue of *S. pistillata*,[33] might be less constrained by the atomic radius differences. The lack of Pb in the crystalline phase raises intriguing questions about the role of ACC in modulating Pb interactions.

Possible contamination sources

Pb contamination in marine environments arises from both natural and anthropogenic sources. In nature, Pb can be introduced through rock weathering and volcano eruptions[40] and occurs in the Earth's crust[15] and soil at an average concentration of 20 mg Pb per kg.[41] Anthropogenic activities, however, have caused elevated levels in coastal waters ranging from 25 ng kg^{-1} in unpolluted regions to 150 ng kg^{-1} in regions impacted by sewage.[42] Though Pb concentrations in northern Red Sea seawater are reported to remain below critical thresholds,[19] higher concentration levels have been reported in sediments and corals in areas exposed to anthropogenic pollution.[43–45]

Elevated Pb levels from anthropogenic disturbances[5,46] pose significant risks to coastal ecosystems, with coral contamination being an indication of unwanted Pb pollution.[47–49] Once released into the ocean, Pb can be transported over long distances by ocean currents.[12] Urban sources, such as metal-rich dust, leaded fuels, industrial waste and possibly contaminated marine vessels, are likely contributors to the Pb detected in corals. Previous reports have identified pollution from sewage[42] and emissions from boats[2] as major sources. Massive shipping activity, especially for oil and petroleum transport, further increases the risk of heavy metal contamination.[50]

In October 2018, dissolved Pb concentration in the Gulf of Aqaba ranged from 0.004 to 0.02 μg L^{-1} following a dust storm.[18] While these levels represent an increase, they remain well below the critical threshold level of 2 μg L^{-1} established by the Australian Water Quality Guidelines for marine environment.[19] Such storms are the likely cause of Pb contamination in our samples.

Although Pb has limited solubility in seawater,[13,51] due to the low solubility of Pb chloride,[52] even small amounts may affect living corals. The detection of Pb in one-month-old coral tissues suggests that minor pollution, possibly from a local dust storm, could have occurred in our study leading to detectable lead accumulation. The source of Pb contamination in our samples, however, remains

unclear. Its presence was discovered incidentally during our investigations, as no Pb sources were known before or during coral treatment. Nevertheless, it is evident that Pb accumulated in the coral tissue while the coral was still alive, prior to sample preparation. These findings highlight the sensitivity of corals as unintentional bioindicators of even low-level Pb contamination.

Effects of Pb on corals

It is estimated that 20% of global coral populations are threatened by exposure to toxic substances.[53] Pb has been shown to impact corals by triggering sublethal effects, such as tentacle retraction in cnidaria and causing the significant loss of their symbionts.[54]

Contamination from heavy metals further disrupts essential physiological processes in marine organisms, including corals, by impairing calcification and lowering photosynthetic efficiency.[55,56] Exposure to metals has been linked to coral bleaching,[57,58] with copper and mercury shown to harm coral symbionts, thereby triggering bleaching events.[59,60] Metal exposure also increases the production of reactive oxygen species, a key factor driving coral bleaching.[61] Furthermore, metals such as copper and zinc can reduce larval survival rates[62] and compromise thermal resilience of *Stylophora pistillata*.[63] Similar synergistic effects are likely for Pb.

While corals can regulate the concentration of various trace elements in the tissue,[2] their sensitivity to the toxic elements increases with higher environmental temperatures. This suggests that the combination of temperature and heavy metals negatively impacts physiological processes, as metals are absorbed more quickly at higher temperatures.[64,65] This raises the need for future investigation, regarding the potential link between toxic heavy metal contamination and coral bleaching.

Conclusions

This study used X-ray fluorescence microbeam mapping, to provide direct evidence that Pb exposure rapidly spreads throughout the soft tissue of living stony corals. Although Pb emissions have decreased in recent decades, our results of thin sections from stony corals, grown in open tanks supplied with seawater through PVC pipes in the Gulf of Aqaba reveal that Pb contamination remains an ecotoxicological threat. The uniform distribution of Pb in coral tissues, coupled with its absence in the skeletal mineral phase, suggests a transient and short-lived or low concentration contamination event, likely caused by a passing ship or dust cloud. Further research is needed to determine the time required for corals to accumulate Pb to the levels we observed, as well as to better understand the effects on the organism, and the rate of Pb incorporation through controlled time-lapse exposure experiments.

Stylophora pistillata and *Pocillopora verrucosa* appear to be unintentional bio-indicators of Pb pollution. While this study did not assess physiological impacts, the findings highlight the importance of addressing heavy metal contamination in marine ecosystems and its broader implications for environmental health.

Given the escalating anthropogenic pressures on coral reefs, particularly in biodiversity hotspots like the Red Sea, proactive measures are essential to

safeguard these ecosystems and the overall health of the marine environment. This may include stricter regulations on Pb emissions, targeted pollution mitigation efforts, and further research to address heavy metal contamination. By detecting and possibly quantifying Pb contamination, this research aims to contribute to the protection of coral reefs and their vital role in supporting marine biodiversity and enhancing climate resilience.

Data availability

The data supporting the findings of this study, including fluorescence maps and Fiji macro, are available at GitHub at **https://doi.org/10.5281/zenodo.14740562**.[66]

Author contributions

Conceptualization: TM and PZ conceptualized and designed the study. Resources: MN grew the corals in the IUI. The beamline scientist IZ set up, aligned and calibrated the beamline. Investigation: KS performed SEM-BEI measurements, and KS, PZ, IZ carried out XRF measurements. Formal analysis and visualization: KS analyzed XRF data and created all figures. MN captured light microscopy images Hagai Nativ (**https://www.hagainativ.com**) collected the underwater pictures of the corals, which is added now (again) in the acknowledgements. Writing – original draft: KS. Writing – review and editing: KS, MN, TM, PZ. Supervision: TM and PZ. Funding acquisition: TM and PZ contributed equally to this paper.

Conflicts of interest

There are no conflicts of interest to declare.

Acknowledgements

References

1 R. Wood, J. E. N. Veron, 1995. Corals in Space & Time. The Biogeography & Evolution of the Scleractinia. xiii + 321 pp. Ithaca, London: Cornell University Press (Comstock). Price US $37.50, £29.50 (paperback). ISBN 0 801 48263 1, *Geol. Mag.*, 1996, **133**, 634, DOI: **10.1017/S0016756800008050**.

2 G. Esslemont, Heavy metals in seawater, marine sediments and corals from the Townsville section, Great Barrier Reef Marine Park, Queensland, *Mar. Chem.*, 2000, **71**, 215–231, DOI: **10.1016/s0304-4203(00)00050-5**.

3 T. P. Hughes, A. H. Baird, D. R. Bellwood, M. Card, S. R. Connolly, C. Folke, R. Grosberg, O. Hoegh-Guldberg, J. B. C. Jackson, J. Kleypas, J. M. Lough, P. Marshall, M. Nyström, S. R. Palumbi, J. M. Pandolfi, B. Rosen and J. Roughgarden, Climate change, human impacts, and the resilience of coral reefs, *Science*, 2003, **301**, 929–933, DOI: **10.1126/science.1085046**.

4 O. Hoegh-Guldberg, P. J. Mumby, A. J. Hooten, R. S. Steneck, P. Greenfield, E. Gomez, C. D. Harvell, P. F. Sale, A. J. Edwards, K. Caldeira, N. Knowlton, C. M. Eakin, R. Iglesias-Prieto, N. Muthiga, R. H. Bradbury, A. Dubi and M. E. Hatziolos, Coral reefs under rapid climate change and ocean acidification, *Science*, 2007, **318**, 1737–1742, DOI: **10.1126/science.1152509**.

5 C. C. Patterson, Contaminated and natural lead environments of man, *Arch. Environ. Health*, 1965, **11**, 344–360, DOI: **10.1080/00039896.1965.10664229**.

6 *End of Leaded Gasoline: World Has Stopped Using Toxic Additive*, NPR, **https://www.npr.org/2021/08/30/1031429212/the-world-has-finally-stopped-using-leaded-gasoline-algeria-used-the-last-stockp**, accessed January 18, 2025.

7 *The History of the Elimination of Leaded Gasoline*, In Custodia Legis, **https://blogs.loc.gov/law/2022/04/the-history-of-the-elimination-of-leaded-gasoline/**, accessed January 14, 2025.

8 D. Seyferth, The Rise and Fall of Tetraethyllead. 2, *Organometallics*, 2003, **22**, 5154–5178, DOI: **10.1021/om030621B**.

9 *The Fuels Campaign*, UNEP – UN Environment Programme, **https://www.unep.org/topics/transport/partnership-clean-fuels-and-vehicles/fuels-campaign**, accessed January 15, 2025.

10 L. Bridgestock, T. Van De Flierdt, M. Rehkämper, M. Paul, R. Middag, A. Milne, M. C. Lohan, A. R. Baker, R. Chance, R. Khondoker, S. Strekopytov, E. Humphreys-Williams, E. P. Achterberg, M. J. A. Rijkenberg, L. J. A. Gerringa and H. J. W. De Baar, Return of naturally sourced Pb to Atlantic surface waters, *Nat. Commun.*, 2016, **7**, 12921, DOI: **10.1038/ncomms12921**.

11 Y. Echegoyen, E. A. Boyle, J. M. Lee, T. Gamo, H. Obata and K. Norisuye, Recent distribution of lead in the Indian Ocean reflects the impact of regional emissions, *Proc. Natl. Acad. Sci. U. S. A.*, 2014, **111**, 15328–15331, DOI: **10.1073/pnas.1417370111**.

12 S. J. S. Flora, G. Flora and G. Saxena, Environmental occurrence, health effects and management of lead poisoning, *Lead Chem. Anal. Asp. Environ. Impact Heal. Eff.*, 2006, 158–228, DOI: **10.1016/B978-044452945-9/50004-X**.

13 B. M. Angel, S. C. Apte, G. E. Batley and M. D. Raven, Lead solubility in seawater: an experimental study, *Environ. Chem.*, 2015, **13**, 489–495, DOI: **10.1071/EN15150**.

14 G. Capodaglio, K. H. Coale and K. W. Bruland, Lead speciation in surface waters of the eastern North Pacific, *Mar. Chem.*, 1990, **29**, 221–233, DOI: **10.1016/0304-4203(90)90015-5**.

15 A. Carocci, A. Catalano, G. Lauria, M. S. Sinicropi and G. Genchi, Lead Toxicity, Antioxidant Defense and Environment, *Rev. Environ. Contam. Toxicol.*, 2016, **238**, 45–67, DOI: **10.1007/398_2015_5003**.

16 R. J. Woosley and F. J. Millero, Pitzer model for the speciation of lead chloride and carbonate complexes in natural waters, *Mar. Chem.*, 2013, **149**, 1–7, DOI: **10.1016/j.marchem.2012.11.004**.

17 A. Botté, C. Seguin, J. Nahrgang, M. Zaidi, J. Guery and V. Leignel, Lead in the marine environment: concentrations and effects on invertebrates, *Ecotoxicology*, 2022, **31**, 194–207, DOI: **10.1007/s10646-021-02504-4**.

18 T. Benaltabet, G. Lapid and A. Torfstein, Seawater Pb concentration and isotopic composition response to daily time scale dust storms in the Gulf of Aqaba, Red Sea, *Mar. Chem.*, 2020, **227**, 103895, DOI: **10.1016/j.marchem.2020.103895**.

19 *ANZECC (1992) water quality guidelines*, 1992, **https://www.waterquality.gov.au/anz-guidelines/resources/previous-guidelines/anzecc-1992**, accessed January 20, 2025.

20 W.-X. Wang, Bioaccumulation and Biomonitoring, *Marine Ecotoxicology*, 2016, ch. 4, pp. 99–119, DOI: **10.1016/B978-0-12-803371-5.00004-7**.

21 C. Copat, F. Bella, M. Castaing, R. Fallico, S. Sciacca and M. Ferrante, Heavy metals concentrations in fish from Sicily (Mediterranean Sea) and evaluation of possible health risks to consumers, *Bull. Environ. Contam. Toxicol.*, 2012, **88**, 78–83, DOI: **10.1007/s00128-011-0433-6**.

22 G. Esslemont, Development and comparison of methods for measuring heavy metal concentrations in coral tissues, *Mar. Chem.*, 2000, **69**, 69–74, DOI: **10.1016/s0304-4203(99)00096-1**.

23 A. Ricolleau, N. Floquet, J. L. Devidal, R. J. Bodnar, J. Perrin, J. Garrabou, J. G. Harmelin, F. Costantini, J. R. Boavida and D. Vielzeuf, Lead (Pb) profiles in red coral skeletons as high resolution records of pollution in the Mediterranean Sea, *Chem. Geol.*, 2019, **525**, 112–124, DOI: **10.1016/j.chemgeo.2019.07.005**.

24 I. Chan, J. J. Hung, S. H. Peng, L. C. Tseng, T. Y. Ho and J. S. Hwang, Comparison of metal accumulation in the azooxanthellate scleractinian coral (*Tubastraea coccinea*) from different polluted environments, *Mar. Pollut. Bull.*, 2014, **85**, 648–658, DOI: **10.1016/j.marpolbul.2013.11.015**.

25 E. J. C. Esper, E. J. C. Esper, *Die Pflanzenthiere in Abbildungen nach der Natur: mit Farben erleuchtet nebst Beschreibungen*, in der Raspischen Buchhandlung, Nèurnberg, 1797, DOI: **10.5962/bhl.title.118730**.

26 J. Ellis and D. C. Solander, *The Natural History of Many Curious and Uncommon Zoophytes: Collected from Various Parts of the Globe*, Printed for Benjamin White and Son… and Peter Elmsly, London, 1786, DOI: **10.5962/bhl.title.64985**.

27 I. Zizak, The mySpot beamline at BESSY II, *J. Large-Scale Res. Facil. JLSRF*, 2016, **2**, A102, DOI: **10.17815/jlsrf-2-113**.

28 C. Schneider, W. Rasband and K. Eliceiri, NIH Image to ImageJ: 25 years of image analysis, *Nat. Methods*, 2012, **9**, 671.

29 W. Demtröder, *Experimentalphysik 3: Atome, Moleküle und Festkörper*, 2005, **https://physik.rptu.de/ags/demtroeder/publications/lehrbuecher**, accessed February 5, 2025.

30 B. L. Henke, E. M. Gullikson and J. C. Davis, X-Ray interactions: photoabsorption, scattering, transmission, and reflection at E = 50-30,000 eV, Z= 1-92, *At. Data Nucl. Data Tables*, 1993, **54**, 181–342.

31 *X-ray Absorption Edge Energies*, **https://www.ruppweb.org/Xray/elements.html**, accessed February 1, 2025.

32 T. Benaltabet, G. Lapid and A. Torfstein, Dissolved aluminium dynamics in response to dust storms, wet deposition, and sediment resuspension in the

Gulf of Aqaba, northern Red Sea, *Geochim. Cosmochim. Acta*, 2022, **335**, 137–154, DOI: **10.1016/j.gca.2022.08.029**.

33 T. Mass, A. J. Giuffre, C. Y. Sun, C. A. Stifler, M. J. Frazier, M. Neder, N. Tamura, C. V. Stan, M. A. Marcus and P. U. P. A. Gilbert, Amorphous calcium carbonate particles form coral skeletons, *Proc. Natl. Acad. Sci. U. S. A.*, 2017, **114**, E7670–E7678, DOI: **10.1073/pnas.1707890114**.

34 S. Al-Rousan, R. Al-Shloul, F. Al-Horani and A. Abu-Hilal, Heavy metals signature of human activities recorded in coral skeletons along the Jordanian coast of the Gulf of Aqaba, Red Sea, *Environ. Earth Sci.*, 2012, **67**, 2003–2013, DOI: **10.1007/s12665-012-1640-0**.

35 A. Godelitsas, J. M. Astilleros, K. Hallam, S. Harissopoulos and A. Putnis, Interaction of Calcium Carbonates with Lead in Aqueous Solutions, *Environ. Sci. Technol.*, 2003, **37**, 3351–3360, DOI: **10.1021/es020238i**.

36 M. P. Andersson, H. Sakuma and S. L. S. Stipp, Strontium, nickel, cadmium, and lead substitution into calcite, studied by density functional theory, *Langmuir*, 2014, **30**, 6129–6133, DOI: **10.1021/la500832u**.

37 A. Sdiri and T. Higashi, Simultaneous removal of heavy metals from aqueous solution by natural limestones, *Appl. Water Sci.*, 2013, **3**, 29–39, DOI: **10.1007/s13201-012-0054-1**.

38 Y. Du, F. Lian and L. Zhu, Biosorption of divalent Pb, Cd and Zn on aragonite and calcite mollusk shells, *Environ. Pollut.*, 2011, **159**, 1763–1768, DOI: **10.1016/j.envpol.2011.04.017**.

39 M. Kirberger and J. J. Yang, Structural Differences Between Pb^{2+}- and Ca^{2+}-binding Sites in Proteins: Implications with Respect to Toxicity, *J. Inorg. Biochem.*, 2008, **102**, 1901, DOI: **10.1016/j.jinorgbio.2008.06.014**.

40 E. N. Edinger, G. V. Limmon, J. Jompa, W. Widjatmoko, J. M. Heikoop and M. J. Risk, Normal Coral Growth Rates on Dying Reefs: Are Coral Growth Rates Good Indicators of Reef Health?, *Mar. Pollut. Bull.*, 2000, **40**, 404–425, DOI: **10.1016/S0025-326X(99)00237-4**.

41 D. B. Smith, W. F. Cannon, L. G. Woodruff, F. Solano, J. E. Kilburn and D. L. Fey, *Geochemical and Mineralogical Data for Soils of the Conterminous United States*, U.S. Geological Survey Data Series 801, 2013, **https://pubs.usgs.gov/ds/801/**.

42 C. Patterson, D. Settle and B. Glover, Analysis of lead in polluted coastal seawater, *Mar. Chem.*, 1976, **4**, 305–319, DOI: **10.1016/0304-4203(76)90017-7**.

43 A.-h. A. M. Ali, M. A. Hamed and H. A. El-Azim, Heavy metals distribution in the coral reef ecosystems of the Northern Red Sea, *Helgol. Mar. Res.*, 2011, **65**, 67–80, DOI: **10.1007/s10152-010-0202-7**.

44 Z. Chase, A. Paytan, A. Beck, D. Biller, K. Bruland, C. Measures and S. Sañudo-Wilhelmy, Evaluating the impact of atmospheric deposition on dissolved trace-metals in the Gulf of Aqaba, Red Sea, *Mar. Chem.*, 2011, **126**, 256–268, DOI: **10.1016/j.marchem.2011.06.005**.

45 A. Torfstein, N. Teutsch, O. Tirosh, Y. Shaked, T. Rivlin, A. Zipori, M. Stein, B. Lazar and Y. Erel, Chemical characterization of atmospheric dust from a weekly time series in the north Red Sea between 2006 and 2010, *Geochim. Cosmochim. Acta*, 2017, **211**, 373–393, DOI: **10.1016/j.gca.2017.06.007**.

46 J. Wu and E. A. Boyle, Lead in the western North Atlantic Ocean: Completed response to leaded gasoline phaseout, *Geochim. Cosmochim. Acta*, 1997, **61**, 3279–3283, DOI: **10.1016/s0016-7037(97)89711-6**.

47 P. S. Rainbow, Trace metal concentrations in aquatic invertebrates: why and so what?, *Environ. Pollut.*, 2002, **120**, 497–507, DOI: **10.1016/s0269-7491(02)00238-5**.

48 R. Chiarelli and M. C. Roccheri, Marine Invertebrates as Bioindicators of Heavy Metal Pollution, *Open J. Met.*, 2014, **04**, 93–106, DOI: **10.4236/ojmetal.2014.44011**.

49 R. Chiarelli, C. Martino and M. C. Roccheri, Cadmium stress effects indicating marine pollution in different species of sea urchin employed as environmental bioindicators, *Cell Stress Chaperones*, 2019, **24**, 675–687, DOI: **10.1007/s12192-019-01010-1**.

50 M. Fine, M. Cinar, C. R. Voolstra, A. Safa, B. Rinkevich, D. Laffoley, N. Hilmi and D. Allemand, Coral reefs of the Red Sea – Challenges and potential solutions, *Reg. Stud. Mar. Sci.*, 2019, **25**, 100498, DOI: **10.1016/j.rsma.2018.100498**.

51 A. M. Beccaria, E. D. Mor, G. Bruno and G. Poggi, Corrosion of Lead in Sea Water, *Br. Corros. J.*, 1982, **17**, 87–91, DOI: **10.1179/000705982798274480**.

52 J. A. Von Fraunhofer, Lead corrosion in sea-water, *Anti-Corros. Methods Mater.*, 1969, **16**, 21–27.

53 M. Spalding, C. Ravilious and E. Green, World atlas of coral reefs, *Choice Rev. Online*, 2001, **39**, 2540, DOI: **10.5860/CHOICE.39-2540**.

54 P. L. Howe, A. J. Reichelt-Brushett and M. W. Clark, Investigating lethal and sublethal effects of the trace metals cadmium, cobalt, lead, nickel and zinc on the anemone *Aiptasia pulchella*, a cnidarian representative for ecotoxicology in tropical marine environments, *Mar. Freshwater Res.*, 2014, **65**, 551–561, DOI: **10.1071/MF13195**.

55 A. D. Harland and B. E. Brown, Metal tolerance in the scleractinian coral *Porites lutea*, *Mar. Pollut. Bull.*, 1989, **20**, 353–357, DOI: **10.1016/0025-326X(89)90159-8**.

56 F. I. Kuzminov, C. M. Brown, V. V. Fadeev and M. Y. Gorbunov, Effects of metal toxicity on photosynthetic processes in coral symbionts, *Symbiodinium* spp, *J. Exp. Mar. Biol. Ecol.*, 2013, **446**, 216–227, DOI: **10.1016/j.jembe.2013.05.017**.

57 S. Wan, X. Yang, X. Chen, Z. Qu, C. An, B. Zhang, K. Lee and H. Bi, Emerging marine pollution from container ship accidents: Risk characteristics, response strategies, and regulation advancements, *J. Cleaner Prod.*, 2022, **376**, 134266, DOI: **10.1016/j.jclepro.2022.134266**.

58 D. R. Bellwood, M. S. Pratchett, T. H. Morrison, G. G. Gurney, T. P. Hughes, J. G. Álvarez-Romero, J. C. Day, R. Grantham, A. Grech, A. S. Hoey, G. P. Jones, J. M. Pandolfi, S. B. Tebbett, E. Techera, R. Weeks and G. S. Cumming, Coral reef conservation in the Anthropocene: Confronting spatial mismatches and prioritizing functions, *Biol. Conserv.*, 2019, **236**, 604–615, DOI: **10.1016/j.biocon.2019.05.056**.

59 R. H. Kayser and R. H. Young, The photoreduction of methylene blue by amines—II. An investigation of the decay of semireduced methylene blue, *Photochem. Photobiol.*, 1976, **24**, 403–411, DOI: **10.1111/j.1751-1097.1976.tb06846.x**.

60 A. Sabdono, Heavy Metal Levels and Their Potential Toxic Effect on Coral *Galaxea fascicularis* from Java Sea, Indonesia, *Res. J. Environ. Sci.*, 2009, **3**, 96–102, DOI: **10.3923/rjes.2009.96.102**.

61 J. L. Dal Pizzol, J. A. Marques, J. da Silva Fonseca, P. G. Costa and A. Bianchini, Metal accumulation induces oxidative stress and alters carbonic anhydrase activity in corals and symbionts from the largest reef complex in the South Atlantic ocean, *Chemosphere*, 2022, **290**, 133216, DOI: **10.1016/j.chemosphere.2021.133216**.

62 A. J. Reichelt-Brushett and P. L. Harrison, The effect of copper on the settlement success of larvae from the scleractinian coral *Acropora tenuis*, *Mar. Pollut. Bull.*, 2000, **41**, 385–391, DOI: **10.1016/S0025-326X(00)00131-4**.

63 G. Banc-Prandi and M. Fine, Copper enrichment reduces thermal tolerance of the highly resistant Red Sea coral Stylophora pistillata, *Coral Reefs*, 2019, **38**, 285–296, DOI: **10.1007/s00338-019-01774-z**.

64 L. S. Hédouin, R. E. Wolf, J. Phillips and R. D. Gates, Improving the ecological relevance of toxicity tests on scleractinian corals: Influence of season, life stage, and seawater temperature, *Environ. Pollut.*, 2016, **213**, 240–253, DOI: **10.1016/j.envpol.2016.01.086**.

65 R. W. Furness and P. S. Rainbow, *Heavy Metals in the Marine Environment*, Amazon.de: Books, **https://www.amazon.de/-/en/Robert-W-Furness/dp/0849355060**, accessed January 20, 2025.

66 K. Sauer, P. Zaslansky and T. Mass, *Experimental XRF data and macros to determine the lead (Pb) distribution in corals*, 2025, DOI: **10.5281/zenodo.14740562**, accessed January 27, 2025.